



ORIGINAL ARTICLE

Multicentury Growth Patterns and Climate Relationships of Three Co-occurring *Nothofagus* Species in High-Elevation Forests of the Valdivian Andes

Claudio Álvarez,^{1,2*} Duncan A. Christie,^{1,2,3*} Álvaro González-Reyes,^{1,4,5,6} Thomas T. Veblen,⁷ Carlos LeQuesne,¹ Juan C. Aravena,^{2,8} Vicente Rozas,⁹ Felipe Flores-Saéz,¹ Moisés Rojas-Badilla,¹ Tania Gipoulou-Zúñiga,¹ and Diego Aliste¹

¹Laboratorio de Dendrocronología y Cambio Global, Instituto de Conservación Biodiversidad y Territorio, Universidad Austral de Chile, Valdivia, Chile; ²Cape Horn International Center for Global Change Studies and Biocultural Conservation (CHIC), O'Higgins 310, Puerto Williams, Chile; ³Center for Climate and Resilience Research (CR)2, Santiago, Chile; ⁴Instituto de Ciencias de la Tierra, Facultad de Ciencias, Universidad Austral de Chile, Valdivia, Chile; ⁵Centro de Humedales Río Cruces CEHUM, Universidad Austral de Chile, Valdivia, Chile; ⁶Centro de Investigación Dinámica de Ecosistemas Marinos de Altas Latitudes - IDEAL, Punta Arenas, Chile; ⁷Department of Geography, University of Colorado Boulder, Boulder, Colorado, USA; ⁸Centro de Investigación Gaia Antártica (CIGA), Universidad de Magallanes, Punta Arenas, Chile; ⁹iuFOR-EiFAB, Área de Botánica, Campus Duques de Soria, Universidad de Valladolid, Soria, Spain

ABSTRACT

Identifying and understanding the response of tree species to climate variability and drought events is a key challenge in addressing climate change in the Andean ecosystems of southern South America.

This study aims to: (1) determine the main temporal patterns of radial growth of three *Nothofagus* species (*N. pumilio*, *N. dombeyi*, and *N. alpina*) on the northwest slope of the Choshuenco volcano, around 40°S, (2) examine the relationship between radial growth and environmental variables, as well as climatic forcings, and (3) evaluate the resilience of these species across an altitudinal gradient in the Valdivian Andes. The chronologies of the three *Nothofagus* species were assessed using principal component analysis, correlation analysis between the chronologies and environmental variables, and resilience analysis for drought years. The *Nothofagus* chronologies reveal an increased common signal in radial tree growth since the 1980s. At the beginning of the growing season (November) all chronologies exhibit a negative relation with precipitation and some chronologies positive relations

Received 28 December 2024; accepted 18 May 2025

Supplementary Information: The online version contains supplementary material available at <https://doi.org/10.1007/s10021-025-00982-9>.

Author Contributions: CA and DC conceived the manuscript and designed the field sampling plan; CA, DC, FF-S, MR-B, TG-Z, and DA collected the samples and performed the laboratory work; CA led the drafting of the manuscript; DC, AG-R, VR, JCA, TV, and CL edited and critically contributed to its writing. All authors approved the final version for publication.

*Corresponding author; e-mail: dendro.alvarez@gmail.com; duncanchristieb@gmail.com

Published online: 25 June 2025

with mean air temperature and the 0 °C isotherm height. These findings suggest that the persistence of snow cover during spring may be crucial for the onset of the tree growth. Previous year hydroclimate appears to have an important role favoring tree growth, with most chronologies exhibiting positive relations with summer soil moisture, and circulation patterns forced by the Antarctic oscillation that favors wet mild and summers. The response to drought varies among species, with *N. alpina* notably exhibiting high resistance, recovery and resilience, likely due to its location near the southern limit of its distribution. Integrating analyses of temporal growth patterns, growth-environment variables relationships, and drought resilience enhances understanding of how *Nothofagus* species have responded to climatic variability in recent decades in the Valdivian Andes forests.

Key words: *Nothofagus*; Climatic variability; Radial growth; Andes; Altitudinal gradient.

HIGHLIGHTS

- Radial growth patterns of three *Nothofagus* species (*N. pumilio*, *N. dombeyi* and *N. alpina*) were analyzed across an altitudinal gradient in the Valdivian Andes.
- Radial growth exhibited a strong common signal since 1980 s, highlighting a shared response to climatic variability.
- Negative correlations with November precipitation and positive correlations with temperature and 0 °C isotherm height indicate snow persistence as a critical factor for growth initiation.

INTRODUCTION

Identifying and understanding the impacts of climatic variability on ecological processes is crucial for effective conservation and management of forest ecosystems, especially in the current context of global change (Arias and others 2021). The observed and projected increases in average air temperature and decreases in precipitation across extensive regions could lead to significant changes in key ecological processes, such as the growth and establishment of tree species (Arias and others 2021). Forest ecosystems, and particularly the performance of tree species, are influenced both

directly and indirectly by climate. These changes may be associated with variations in temperature and precipitation patterns, as well as disruptions in disturbance regimes, such as landslides triggered by intense and episodic precipitation events and heatwaves that increase the risk of fires, factors that influence tree growth and dynamics (Seidl and others 2017; González-Reyes and others 2023). Among the forest ecosystems that have experienced the most significant alterations in their ecological processes are high-altitude forests, which represent the altitudinal limits of tree distributions in mountainous landscapes around the world.

In the southern Andes of South America, specifically in central-southern Chile (35°S–55°S), there is an extensive area of high-altitude forests dominated by species of the genus *Nothofagus*. At the upper altitudinal limit, *Nothofagus pumilio* (Lenga) is the predominant species (Donoso 1993), which has been widely studied in dendroclimatic research (Villalba and others 1997; Lara and others 2001, 2005; Daniels and Veblen 2004; Srur and others 2008; Álvarez and others 2015; among others). In Andean forests situated below 1000 m a.s.l., *Nothofagus dombeyi* (Coigue) and *Nothofagus alpina* (Raulí) are found, and these species have also been investigated through dendrochronological studies in northern Patagonia ca. 40°S on the eastern slope of the Andes (Suarez and others 2004, 2015; Bonada and others 2022a).

The growth of *Nothofagus* species in the temperate Andes is influenced by both precipitation and temperature, with moisture availability primarily controlling growth in more humid regions and temperature acting as a limiting factor in drier or warmer environments. Precipitation plays a key role in the radial growth of *Nothofagus* in the temperate Andes. In *N. pumilio*, Villalba and others (1997) found a positive and significant correlation between growth and September precipitation, while the late spring and early summer precipitation (November and December) showed a negative relationship with growth. Along a latitudinal gradient (36°S–55°S), Lara and others (2005) found a positive correlation between precipitation and growth in the northern part of the species distribution range. In *N. dombeyi*, the positive relationship between growth and precipitation has been documented along a longitudinal precipitation gradient near 40°S, suggesting that higher moisture availability favor its growth (Suarez and others 2015). In populations located in drier areas east of the Andes, severe droughts have led to high mortality rates, highlighting the species dependence on water availability (Suarez and others 2004). Simi-

larly, in *N. alpina*, summer precipitation has a positive impact on radial growth. Studies in mixed forests with *N. obliqua* along a longitudinal gradient near 40°S have confirmed the reliability of *N. alpina* growth rings for dendroclimatic studies, showing that its growth is greater in more humid environments on the eastern slope of the Andes (Bonada and others 2022a, 2022b). The effect of temperature on the growth of *Nothofagus* varies depending on the geographic location and species. In *N. pumilio*, Lara and others (2005) found a negative correlation between growth and temperature in the northern part of its latitudinal range (36°S–55°S), while in the southern part, growth showed a positive correlation with mean annual temperature. In the case of *N. dombeyi*, a negative relationship between growth and temperature during the growing season has been documented, indicating that warmer temperatures may limit its development (Suarez and others 2015). On the other hand, in *N. alpina*, a negative correlation between growth and summer temperatures has been identified, suggesting that higher temperatures may reduce the growth rate of the species (Bonada and others 2022b). This reinforces the idea that the growth of *N. alpina* is influenced by both water availability and temperature, with a preference for cooler and wetter environments on the eastern slope of the Andes.

Despite extensive research on the relationship between climate and growth for the three *Nothofagus* species individually, no study has examined sites where these species coexist in their respective altitudinal zones under a common climatic regime on the western slope of the Andes. In this context, the northwestern slope of the Choshuenco volcano, where these *Nothofagus* species coexist, offers an ideal setting for such a study. This area has experienced minimal human intervention due to its location within a national reserve, with large ravines that limit access, and a long period of volcanic inactivity, with the last eruptions recorded in 1822 (Caldcleugh 1836) and 1864 (Vidal Gormaz 1869). These unique conditions make it an exceptional site to examine the relationship between the radial growth of *Nothofagus* and environmental variables across an altitudinal gradient.

Previous dendroclimatic studies in this area have identified significant relationships between radial growth and climate. At the treeline (ca. 1400 m), *N. pumilio* growth was negatively correlated with November–December precipitation and positively correlated with average temperature from November to January (Álvarez and others 2015).

At the lower boundary of the *N. pumilio* ecotone (ca. 1100 m altitude), radial growth exhibited a significant negative relationship with February maximum temperature and November precipitation (Serrano-León and Christie 2020). However, these studies only included data up to 2010, excluding the recent extreme drought years that began in 2010 in central-southern Chile (González-Reyes and Muñoz 2013; Garreaud and others 2017; González-Reyes and others 2020).

Drought events have become increasingly frequent from 2010 to the present in central-southern Chile (Garreaud and others 2017; González-Reyes and others 2020), causing significant impacts on tree growth, including high mortality rates (Suarez and others 2004; Rodríguez-Catón and others 2016). These effects are expected to intensify in the coming decades due to ongoing global climate change (Trenberth and others 2014). To assess the impact of drought stress on tree growth, the concepts of resistance, recovery, and resilience (sensu Lloret and others 2011) provide valuable insights. Resistance measures the potential reduction in radial growth during a drought compared to pre-drought conditions. Recovery measures the average growth following the drought event, while resilience evaluates the ability of radial growth to recover after a disturbance by calculating the ratio between average growth in the years following the drought and the average growth in the preceding years (Lloret and others 2011). Drought responses using these indices have been previously evaluated in central and central-southern Chile, in mediterranean region, transition zones between the mediterranean and temperate regions, as well as in lower-altitude areas (Urrutia-Jalabert and others 2021; Venegas-González and others 2022; Rojas-Badilla and others 2023). However, these responses have not been analyzed at the upper limit of the three *Nothofagus* species studied in the Andes, leaving a gap in understanding their vulnerability under changing climate conditions.

To expand on previous findings, this study incorporates additional environmental variables not previously considered in studies on Choshuenco volcano. These include soil moisture (McNally and others 2017), derived from satellite measurements and climate reanalysis (Martens and others 2017), and the 0 °C height of isotherm, which defines the altitude of the snow line and differentiates areas receiving liquid versus solid precipitation (Minder and others 2011). Additionally, vapor pressure deficit (VPD), a key factor in regulating stomatal conductance and thereby influencing radial growth (Treydte and others

2014), is evaluated to better understand the responses of these species to climatic variability. These variables provide a broader perspective on how *Nothofagus* species on the northwestern slope of the Choshuenco volcano have been responding to recent climate variability, particularly under prolonged drought conditions.

The primary aim of this research is to investigate the climatic and environmental signals of three co-occurring *Nothofagus* species given by *N. pumilio*, *N. dombeyi*, and *N. alpina* growth using a network of five ring-width chronologies across an altitudinal gradient on the Choshuenco volcano in the Valdivian Andes of northern Patagonia (40°S). The specific objectives are: (a) to identify the main temporal patterns of radial growth in these high-elevation *Nothofagus* species, (b) to analyze the relationship between radial growth and both environmental variables and climatic drivers on a monthly and seasonal scale, and c) to evaluate resistance, recovery, and resilience of radial growth in response to four drought events across the altitudinal gradient in the Valdivian Andes.

MATERIAL AND METHODS

Study Area

The Valdivian temperate Andes (~ 40°S) feature peaks that typically reach altitudes between 2000 and 2700 m (Figure 1A, B). The soils are andosols, developed from volcanic ash (Daniels and Veblen 2003). Under forests cover, these soils are characterized by an Ah horizon rich in organic material. They also contain abundant allophane, which contributes to slope instability. These soils generally have a high pore volume and high water infiltration rates, resulting in low retention capacity (Hildebrand-Vogel and others 1990). The study area is located along an altitudinal gradient within a National Forest Reserve on the northwestern slope of the Choshuenco volcano, and is largely free of recent human activity. The studied species correspond to *N. pumilio* forests growing at higher elevations near the treeline (between 1200 and 1400 m altitude), *N. dombeyi* around 1100 m, and *N. alpina* near 1000 m, both at the upper limits of their altitudinal distribution (Figure 1C). In the higher-altitude sites where *N. pumilio* grows, there was no evidence of disturbances from volcanic ash falls or lava flows. Sites with evidence of avalanches were excluded from sampling. In the lower-altitude (ca. 1000 m) areas where *N. alpina* predominates, no recent logging evidence, such as stumps, was found. However, low tree density and

dense thickets of *Chusquea culeou* were observed, suggesting past selective logging interventions, though no recent logging was evident.

The primary climatic influences in south-central Chile (38°S–2°S) in the study area are the subtropical Pacific anticyclone and the prevailing westerly winds from the Pacific Ocean. The interaction between these factors explains the seasonality of precipitation and temperature in this region (Garreaud and others 2009). During winter (June–August), the subtropical Pacific Anticyclone shifts north (35°S–40°S), increasing precipitation. Conversely, in summer (December–March), the anticyclone moves between 40°S–45° S, diverting westerly storm flows to higher southern latitudes, resulting in low precipitation in mid-latitudes (Aceituno 1988). Precipitation in the study area shows a marked altitudinal gradient, from 2000 mm annually at lower altitudes up to 4000 mm near the treeline. This precipitation is concentrated in winter months (June, July, and August) and falls as snow above 1000 m. The average annual temperature is around 10 °C, with July being the coldest month (average 6.8 °C) and January the warmest (average 16.5 °C). At the interannual time-scale, the regional climate is modulated by both the Antarctic Oscillation (AAO) also known as the Southern Annular Mode (SAM), and to a lesser extent the El Niño-Southern Oscillation (ENSO; Garreaud and others 2009; Christie and others 2011). The AAO is the principal mode of atmospheric circulation variability in the extratropics of the Southern Hemisphere (Thompson and Wallace 2000). Positive phases of the AAO are associated with decreased geopotential heights over the Antarctica, increased geopotential heights over the mid-latitudes, a poleward shift of the storm track, and a strengthening of the polar vortex, resulting in warmer and drier conditions over our study region during summer (Christie and others 2011). The opposite conditions occur during negative AAO phases (Thompson and Wallace 2000; Fyfe 2003).

Tree Species

Species of the genus *Nothofagus* dominate the high-altitude forests of the temperate Valdivian Andes. *N. pumilio* is prominent at the upper forest line, with an extensive latitudinal range between 35°S and 55°S along the Andes of Chile and Argentina (Donoso 1993; Veblen and others 1996). This deciduous tree species can reach 30 m in height, 1.7 m in diameter, and attain ages of 400 years (Donoso 1974; Rebertus and Veblen 1993; Villalba and others 2003). *N. pumilio* forms pure stands or

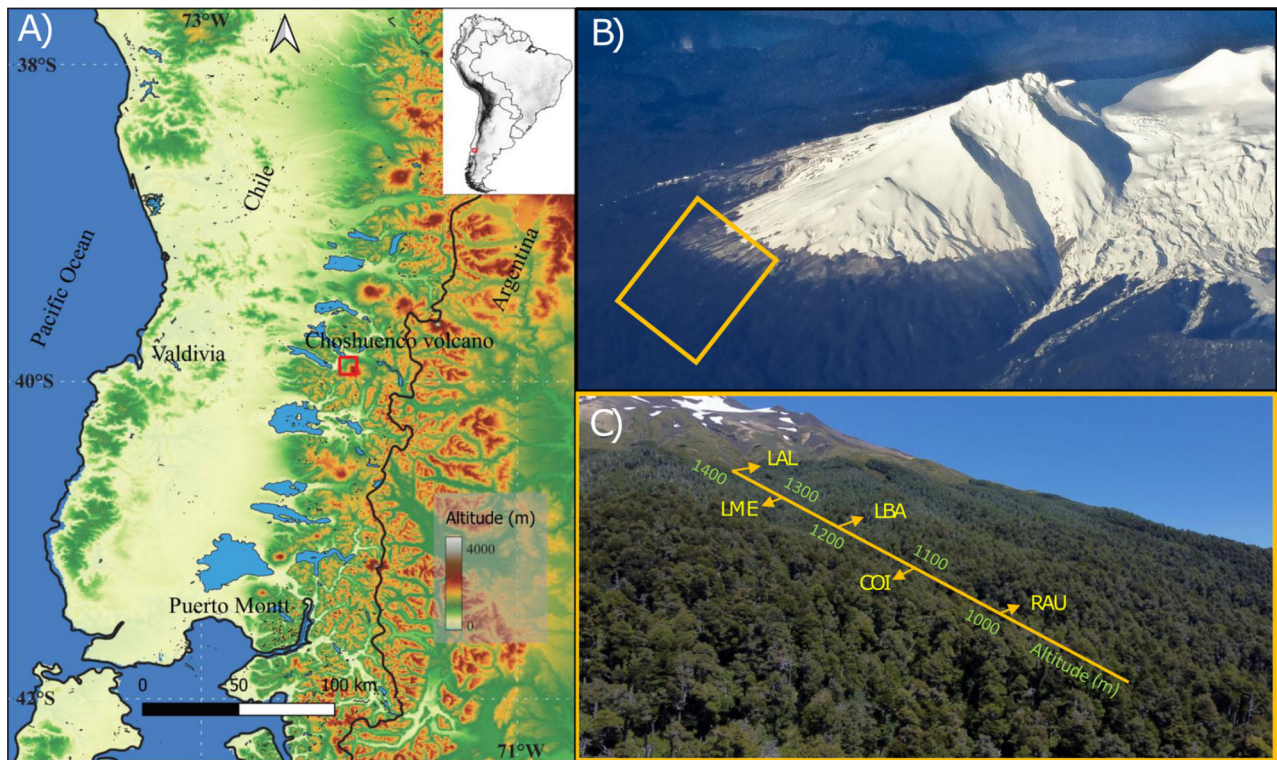


Figure 1. **A** Location of Choshuenco volcano (red rectangle) near 40°S on the western slope of the Andes in southern South America. **B** Panoramic view of the northwestern slope of Choshuenco volcano, with the orange rectangle indicating the section of the altitudinal transect studied in the *Nothofagus* forests. This panoramic picture was taken in winter when *Nothofagus pumilio* loses its leaves, which is why the upper part of the altitudinal transect appears grayish. **C** Altitudinal transect of the chronologies developed on the northwestern slope of Choshuenco volcano, ranging from 1400 to 1000 m in elevation: three sites of *N. pumilio*—LAL (high elevation), LME (mid-elevation), and LBA (low-elevation). COI: *N. dombeyi*, and RAU: *N. alpina*.

associates with species like *Araucaria araucana*, *N. antarctica*, *N. dombeyi*, and *N. betuloides* (Veblen and others 1996).

N. dombeyi (Coigue) is an evergreen species occurring in the temperate Valdivian Andes, with a range from 34°S to 48°S on the western slope of the Andes (Donoso 1974). It can reach 4 m in diameter and 38–45 m in height (Donoso 1974). *N. dombeyi* typically occupies the dominant upper canopy layer, with a maximum lifespan of 500–600 years (Veblen and others 1996). It is a shade-intolerant species that regenerates primarily after large-scale disturbances, such as volcanic eruptions and landslides caused by earthquakes and to a lesser extent from fires and wind blowdowns (Donoso 1993). Finally, the third species studied is *N. alpina*, a deciduous tree that grows in Andean environments from 35°S to 40°S. *N. alpina* (Raulí) can reach diameters of up to 3 m and heights of 35–40 m (Donoso and others 1986). The environment where this species grows is characterized by precipitation ranging from 1500 to 4000 mm in Chile

and southwestern Argentina. Most locations experience a summer dry period (December–March) lasting at least three months. This species grows on deep, well-drained, and fertile soils derived from volcanic ash and tends to avoid topographic depressions prone to cold air pockets (Burschel and others 1976; Veblen and others 1996).

Tree-ring Chronologies Development

To construct the chronologies for *N. pumilio*, wood samples were collected from at least 30 individuals with trunk diameters over 20 cm at three different altitudes in 2012: low (approximately 1200 m; LBA), middle (1300 m; LME), and high (1400 m; LAL). For *N. dombeyi*, samples were taken from 30 individuals at around 1100 m (COI). A second collection of samples was conducted in the austral summer of 2021 to update the chronologies to 2019. During this time, wood samples from 19 *N. alpina* individuals were collected at around 1000 m (RAU), representing the altitudinal limit of species in the study area (Figure 1C). Increment borers

were used to extract 5 mm diameter wood cores. Subsequently, these cores were mounted on wooden frames and sanded with increasingly fine sandpaper to clearly reveal the growth ring boundaries. The rings were then dated according to the Southern Hemisphere convention by Schulman (1956), which assigns each growth ring to the calendar year when growth began. Afterward, ring widths were measured under a microscope using a Velmex measuring system (Velmex Inc., Bloomfield NY, USA) with a precision of 0.001 mm. The samples were cross-dated using the COFECHA software, which verifies accurate dating through correlation analysis of the ring-width series (Holmes 1983). The accurately dated ring-width series were then standardized using a negative exponential curve with the ARSTAN software (Cook and Holmes 1984), allowing the removal of growth trends unrelated to climatic variability (Fritts 1976). This procedure standardizes the ring-width series, reduces variance among samples, and converts them into dimensionless index values. The quality of the chronologies was assessed using the expressed population signal (EPS), which estimates how closely a mean chronology from a finite number of trees approximates a theoretically perfect chronology from a finite number of trees (Cook and others 1990). To calculate EPS, we used a 50-year window with a 25-year overlap between adjacent windows. Finally, the ARSTAN software was used to generate the standard version of the ring-width chronologies for *N. pumilio*, *N. dombeyi*, and *N. alpina*, reflecting the annual variations in radial tree growth (Cook and others 1990).

Climate Data

To evaluate the relationships between the standardized chronologies and environmental variables, we used precipitation data from CR2 Met, which has a spatial resolution of $0.05^\circ \times 0.05^\circ$, covering the period from 1981 to 2019 (<https://ma.wun.cr2.cl/>). Air temperature data at 2 m above ground level were obtained from ERA5, with a spatial resolution of $0.25^\circ \times 0.25^\circ$ <https://cds.climate.copernicus.eu/cdsapp#!/dataset/reanalysis-era5-single-levels-monthly-means?tab=overview>, spanning from 1959 to 2019 (Hersbach and others 2020). Additionally, we used soil moisture data obtained from the Famine Early Warning Systems Network Land Data Assimilation System (FLDAS; McNally and others 2017). This global land surface model is driven by various datasets from satellite measurements and atmospheric analyses, which are evaluated using direct comparisons of outputs

with independent measurements (ground/satellite) and indirect comparisons, including correlations of soil moisture with vegetation indices (McNally and others 2017). The FLDAS data provide monthly gridded soil moisture data at various depths, with a horizontal resolution of approximately 10 km since the year 1982. The data are expressed as the volume of water per soil volume (m^3/m^3). For our research, we focused on the soil moisture layer between 0–10 cm. We used gridded ($0.5^\circ \times 0.5^\circ$) mean monthly temperature and relative humidity data obtained from the Climate Research Unit (CRU) (https://climexp.knmi.nl/selectfield_obs2.cgi?id=someone@somewhere; Harris and others 2020) to calculate VPD. First, we calculated saturation vapor pressure e_s in millibars using the equation developed by Hartmann (2016).

$$e_s = 6.11 * \exp\left(\frac{L}{R_v} \left(\frac{1}{273} - \frac{1}{T}\right)\right)$$

where L represents the latent heat of evaporation ($2.5 \times 10^6 \text{ J kg}^{-1}$), R_v is the gas constant for water vapor ($461 \text{ J K}^{-1} \text{ kg}^{-1}$), and T is the temperature in degrees Kelvin. Based on the e_s , VPD was calculated using the equation:

$$\text{vpd} = \frac{e_s * (100 - \text{RH})}{100}$$

where RH represents the relative humidity in percentage. For the variables in cell format, although the spatial resolution of the grids varies depending on the variable, all the environmental variables were extracted from a single cell. For the extraction of the data grid, we used the ncdf4 package in R.

The 0°C isotherm height data were obtained from monthly radiosonde observations at the Tepual airport station in Puerto Montt (Dirección Meteorológica de Chile) and cover the period from 1958 to 2019. To calculate the correlations between the radial growth of *Nothofagus* species and the climatic forcings of the El Niño Southern Oscillation (ENSO) and Antarctic Oscillation (AAO), the SST 3.4 index (<https://www.cpc.ncep.noaa.gov/data/indices/ersst5.nino.mth.91-20.ascii>) and the AAO-Marshall index (<http://www.nerc-bas.ac.uk/icd/gjma/sam.html>; Marshall 2003) were used.

Temporal Patterns of Chronologies Variability and Climate Relationships

To identify similarities in the radial growth patterns of the five chronologies developed for *N. pumilio*, *N. dombeyi*, and *N. alpina*, a principal component analysis (PCA) was performed on the standard chronologies for the common period from 1900 to

2019. The sampling unit in this analysis was the standard chronologies. The relationship between the first principal component (PC1) and environmental variables was assessed by calculating correlation functions between PC1 and the detrended environmental variables. An autoregressive model was applied to the series to remove the autocorrelation trend from environmental variables.

To evaluate the temporal variation of the common signal in radial growth, PCA was conducted on the five standard chronologies, each covering the common period from 1900 to 2019. In this case, the sampling unit was the standard chronologies of each species. Thirty-year moving windows (89 windows) with a 29-year overlap were applied to the ring-width indices of each chronology. Finally, the percentage of variance explained by each PCA was plotted for the central year of each interval. The PC1 loading values for each chronology were extracted for the periods defined by significant regime shifts in the explained variance, as identified using the Rodionov (2004) method with a 95% confidence level. For each of these periods, the positive loadings of the chronologies on PC1 were graphically represented.

Tree Growth and Its Relationship with Regional and Large-scale Climate

To examine the relationships between monthly climate variables, climatic forcing indices, and standard *Nothofagus* tree ring-width chronologies, we performed correlation functions using the standardized chronologies as the sample unit. These five chronologies were correlated with monthly instrumental records of mean temperature (ERA5), 0 °C isotherm height (DMC), vapor pressure deficit (VPD, CRU derived), Precipitation (CR2Met), soil moisture (FDLS), Antarctic Oscillation Index (AAO) using the treeclim package in R (Zang and Biondi 2015). Since radial growth often shows significant correlations with the climatic conditions of the year preceding ring formation (Fritts 1976), we conducted correlation analyses over a 21-month period, from August of the previous growing season to April of the current growing season. Before computing the correlation functions, environmental variables and indices were detrended using an autoregressive model to remove temporal trends.

To assess the relationship between the main mode of *Nothofagus* forest tree growth on the Choshuenco volcano and large-scale climate patterns and variations, we performed correlation maps using the first principal component (PC1) of

radial growth as the sampling unit. PC1 was derived from a principal component analysis (PCA) of the five standard *Nothofagus* chronologies. Correlations were calculated between the PC1 amplitudes and the NCEP $2.5^\circ \times 2.5^\circ$ gridded data sets of previous summer (January–March) 600 mb zonal wind and 800mb geopotential height for the period 1948–2019 (Kistler and others 2001).

Drought Resilience Analysis

To assess the resilience of radial growth in the three *Nothofagus* species studied during and after drought events, resistance, recovery, and resilience indices were calculated according to the methodology of Lloret and others (2011). For this study, resistance is defined as the reduction in radial growth following a disturbance, measured by comparing the growth of individual trees during droughts to the average growth over the four preceding years. Recovery evaluates the growth after four years following the drought event. The resilience index measures the ability of radial growth to recover after a disturbance, calculated as the ratio between the average growth during the four years following the drought and the average growth during the four years preceding it.

For these analyses, raw ring-width of the individual trees was used due to the lack of a general trend that could suggest an age effect during the drought years studied. The resistance, recovery, and resilience indices were calculated using the `res.comp` function from the `pointRes` package in R (Van der Maaten-Theunissen and others 2015). A resistance value of less than 1 indicates reduced resistance, while a recovery value greater than 1 suggests that growth has recovered compared to the growth level during the drought year. Conversely, a resilience value greater than 1 indicates either complete recovery or increased growth compared to the growth level over the four years preceding the drought year (Gazol and others 2017).

Drought events were identified based on the self-calibrated Palmer Drought Severity Index (scPDSI TS4.05) data (<https://crudata.uea.ac.uk/cru/data/drought/>; Barichivich and others 2021). These data were extracted for the coordinates 39.9°S , 72.07°W , corresponding to the sampled area on the northwest slope of Choshuenco Volcano, using the `ncdf4` package in R (Pierce 2024). The scPDSI is an enhanced index that reflects soil moisture conditions by accounting for atmospheric moisture inputs and soil evaporation (Wells and others 2004). To identify drought events, scPDSI data were

averaged over the growing season from October to March. Periods with scPDSI values below -1.6 during these months were classified as moderate droughts (specifically, the years 1983, 1988, 1996, and 1998, Figure S1).

Individual Tree-Ring Analysis at Tree Level

To explore individual tree growth patterns of trees from the three co-occurring *Nothofagus* species across the elevation gradient according by the main growth pattern of the whole *Nothofagus* community ($n = 497$ trees), we developed multi-species tree-ring chronologies derived from tree-ring series from the four *Nothofagus* individuals significantly, and non-significant correlated ($p < 0.95$) with the

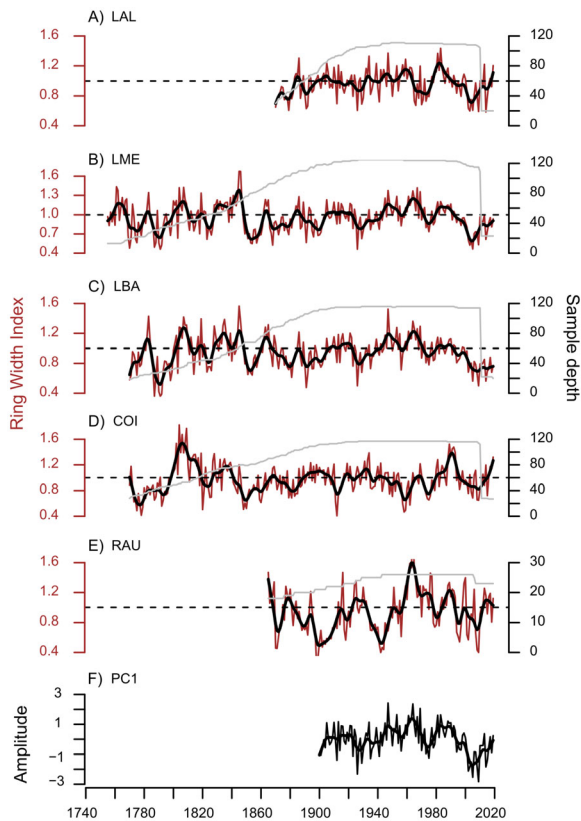


Figure 2. Standard chronologies of *Nothofagus pumilio* showed an EPS > 0.85 . **A** LAL (high-elevation), **B** LME (mid-elevation), **C** LBA (low-elevation). **D** Standard chronology of *Nothofagus dombeyi* (COI), and **E** *Nothofagus alpina* (RAU), **F** PC1 calculated from five chronologies studied. The horizontal dashed line represents the mean value of the Ring Width Index, while the gray line shows the number of series included in each chronology. The solid black line is a 10-year spline applied to each standard chronology and PC1.

amplitude of the PC1 derived from the five chronologies of the study sites (Figure 2F).

To quantify the number of trees that exhibited growth reduction versus those that did not, we analyzed individual series from five standard chronologies and PC1 scores over the period 1900–2019. Correlations were calculated between each series and PC1, classifying them based on their significance at the 95% confidence level, using the critical r -value for the common period. Based on this classification (correlated and uncorrelated series), annual means of ring-width indices were computed for each group. For each multi-species derived chronologies we calculated the proportion of individuals of each species contribution expressed in relative percentages (%). The Rodionov regime-change detection test was then applied to detect significant shifts in the mean (95% confidence level). Finally, we calculated indices de resistance, recovery, and resilience according to Lloret and others (2011) for each multi-species chronologies with respect to the drought events of 1983, 1988, 1996 and 1998 (see Figure S1), and significant differences of the indices between both groups were assessed using the non parametric Mann–Whitney U test.

RESULTS

Ring-Width Chronologies of *N. pumilio*, *N. dombeyi*, and *N. alpina*

This study developed and updated three standard ring-width chronologies for *N. pumilio* at high, mid, and low altitudes, as well as one standard chronology for *N. dombeyi* and one for *N. alpina*. The *N. pumilio* and *N. dombeyi* chronologies included more than 100 series each, while the *N. alpina* chronology included 26 series (Table 1). The *N. pumilio* chronologies, with EPS values greater than 0.85 (Figure 2A–C), showed a strong common signal and cover the periods 1870–2019, 1755–2019, and 1770–2019, respectively. For *N. dombeyi*, the period with EPS > 0.85 spans from 1770 to 2019 (Figure 2D), and for *N. alpina*, it extends from 1865 to 2019 (Figure 2E). Correlation values among the series within each chronology ranged from 0.48 for high *N. pumilio* and *N. alpina* forests to 0.53 for *N. pumilio* mid-altitude and *N. dombeyi* forests (Table 1, Figure 2). Over the last 120 years, similar growth patterns were observed between *N. pumilio* at high, mid, and low altitudes, with the three chronologies showing comparable growth curves and a significant decline in growth after 1990. After 2010, growth increased in *N. pumilio* at

Table 1. Statistics Parameters of the Chronologies *Nothofagus pumilio* (LAL: high-elevation; LME: mid-elevation; and LBA: low-elevation), *N. dombeyi* (COI) and *N. alpina* (RAU) on the Western Slope of the Volcano Choshuenco.

Site	LAL	LME	LBA	COI	RAU
Series intercorrelation	0.48	0.53	0.52	0.53	0.48
Mean ring width (mm) ± sd	1.30 ± 0.66	0.93 ± 0.47	0.99 ± 0.50	1.24 ± 0.66	1.08 ± 0.70
Mean sensitivity	0.32	0.31	0.30	0.30	0.31
Number of trees	93	116	112	110	15
Number of series	111	128	123	119	26
Time span (> 5 series)	1814–2019	1710–2019	1669–2019	1635–2019	1775–2019
Missing rings (%)	0.06	0.07	0.06	0.07	0.22
First-order autocorrelation	0.62	0.67	0.69	0.72	0.75
Altitude (m)	1400	1300	1200	1100	1000
Time span with EPS (> 0.85)	1870	1755	1770	1770	1865

high and *N. pumilio* at medium altitude, while it remained stable in *N. pumilio* low altitude (Figure 2C). *N. dombeyi* exhibited a growth curve that remained near or below the mean from 1900 until the mid-1980s, followed by a substantial increase in the 1990s. Subsequently, growth showed a slight decline from the mid-2000s to the mid-2010s, followed by an increase from the mid-2010s to 2019. *N. alpina* exhibited the greatest variability in its growth curve among the three species analyzed, with growth below average from 1860 to 1960. A growth peak was observed in the mid-1960s, followed by a decreasing trend that remained slightly below the mean from the mid-1990s to 2010. Subsequently, an increase in growth was observed after 2010.

As expected, the highest correlation values were found among the *N. pumilio* chronologies, with a particularly strong correlation between the low- and mid-altitude sites ($r = 0.92$, $p < 0.01$) during the common period from 1900 to 2019. Significant correlations were also observed between species, such as *N. alpina* and *N. pumilio* mid-altitude ($r = 0.34$, $p < 0.05$), *N. alpina* and *N. pumilio* low altitude ($r = 0.34$, $p < 0.05$), *N. dombeyi* and *N. pumilio* high altitude ($r = 0.22$, $p < 0.05$) and *N. dombeyi* and *N. pumilio* mid-altitude ($r = 0.18$, $p < 0.05$). However, no significant correlation was found between the *N. dombeyi* and *N. alpina* chronologies (Figure 3).

The PCA calculated using moving windows revealed two main growth patterns (PC1 and PC2), which explained 54% and 20% of the variability, respectively. These patterns remained stable at around 50% and 25%, respectively, until approximately 1980. After 1980, there was a sharp increase in PC1 values, exceeding 65% until 2004,

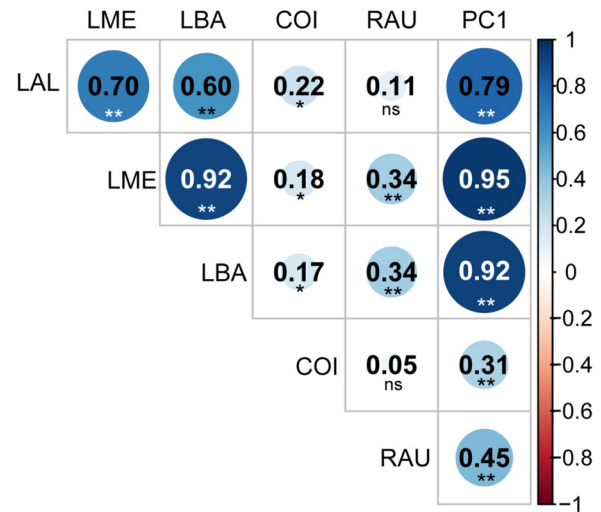


Figure 3. Pearson correlation coefficients between the standard chronologies of five *Nothofagus* species sites on the northwestern slope of Choshuenco volcano. The correlation analysis was calculated for the period 1900–2019. Three sites of *N. pumilio*: LAL = high-elevation, LME = mid-elevation, LBA = low-elevation. *N. dombeyi*: COI, and *N. alpina*: RAU (* $P < 0.05$; ** $P < 0.01$).

while PC2 experience a marked decline, reaching values close to 15% (Figure 4).

Relationship Between Radial Growth and Environmental Variables

For the correlation analysis between the radial growth of the *Nothofagus* chronologies, along with the PC1 calculated for the common period from 1900 to 2019, the following variables were considered: mean temperature (Tmean), 0 °C isotherm height (IsoT), vapor pressure deficit (VPD), precipitation (Pp), soil moisture (SM; 0–10 cm), and

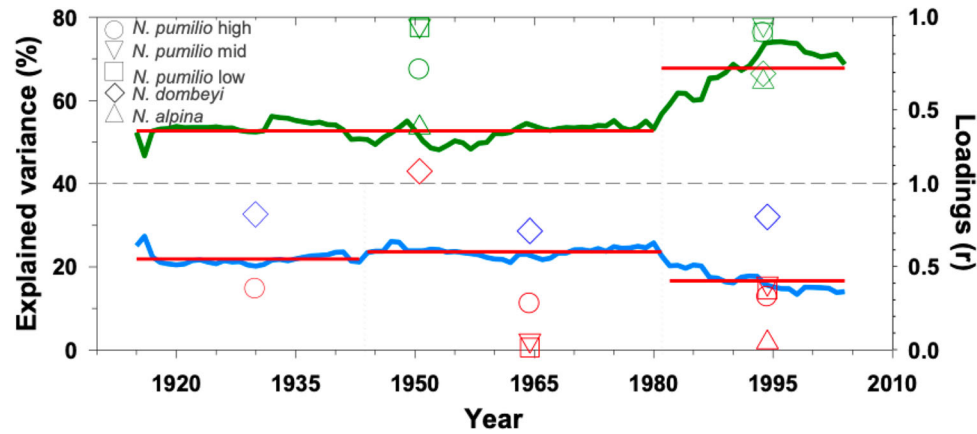


Figure 4. Temporal variation of the common signal in tree growth between the five analyzed *Nothofagus* tree-ring chronologies during the 1900–2019 common period, explained by a 30-year moving window principal component analysis (PCA) of the respective tree-ring chronologies. The green and light-blue lines indicate the percentage (%) of the explained variance of the PC1 and PC2, respectively, of the running PCA developed for 30-year moving windows with a 29-year overlap and plotted on the centroid + one year for each window. The horizontal red lines show significant (95% CL) regime shifts in the time series utilizing the Rodionov (2004) method (window length = 30 years) and the vertical dotted lines highlights significant regime shifts in the respective moving explained variance (%) of each PC. Symbols (circle, diamond, and triangles) indicates the respective loadings of each tree-ring chronology to a PC1 and PC2 amplitudes of a PCA of the five three-ring chronologies for the period 1900–2019, during each significant regime period of explained variance. For PC2, only symbols indicating positive loadings are plotted. Red symbols indicate non-significant ($p < 0.01$) correlation between the respective tree species chronology and the corresponding PC amplitude during the regime shift period.

the climatic forcing indices El Niño Southern Oscillation (ENSO) and Antarctic Oscillation (AAO; Figure 5). Environmental variables related to temperature showed positive correlations with growth during the current growing season (Figure 5A–C). Notably, *N. pumilio* high altitude showed significant positive correlations ($p < 0.01$) between its growth and mean temperature (Tmean), the 0 °C isotherm height (IsoT), and vapor pressure deficit (VPD) in December. *N. pumilio* mid-altitude, *N. pumilio* low altitude, and *N. alpina* also exhibited significant positive correlations ($p < 0.05$) with November Tmean. The IsoT for November showed significant positive correlations ($p < 0.05$) with *N. pumilio* high altitude and mid-altitude, *N. dombeyi*, and PC1. Conversely, IsoT revealed significant negative correlations with *N. alpina* growth ($p < 0.01$) in December and February. Additionally, a positive correlation was found between *N. alpina* growth and November VPD ($p < 0.05$). Interestingly, significant negative correlations between radial growth and temperature-related variables dominate in December of the previous growing season (Figure 5A–C). A notable shift in *N. alpina* was observed, with a positive correlation ($p < 0.01$) between radial growth and the previous November Tmean transitioning to a significant negative cor-

relation in December and March of the same previous growing season ($p < 0.01$).

The strongest correlations were negative and occurred between all chronologies, PC1, and November precipitation during the current growing season ($p < 0.01$). Additionally, *N. dombeyi* growth showed a positive correlation with December precipitation and a negative correlation with August and January precipitation during the current growing season ($p < 0.05$; Figure 5D). Previous season soil moisture (SM) was positively correlated with radial growth in most of the species analyzed. Specifically, *N. pumilio* low, *N. dombeyi*, and radial growth ($p < 0.05$) showed positive correlations with SM from December to April in the prior season (Figure 5E). Finally, no significant correlations were observed with the SST 3.4 index of the ENSO climate driver. However, there were correlations with the AAO-Marshall index, which were mainly negative during the summer months of the previous growing season. Negative correlations were found between January AAO and the radial growth of *N. pumilio* mid-altitude and low altitude, *N. alpina*, and PC1 ($p < 0.05$). In contrast, positive correlations were observed between the growth of *N. pumilio* high altitude, *N. dombeyi*, and November AAO during the current growing season ($p < 0.05$; Figure 5F).

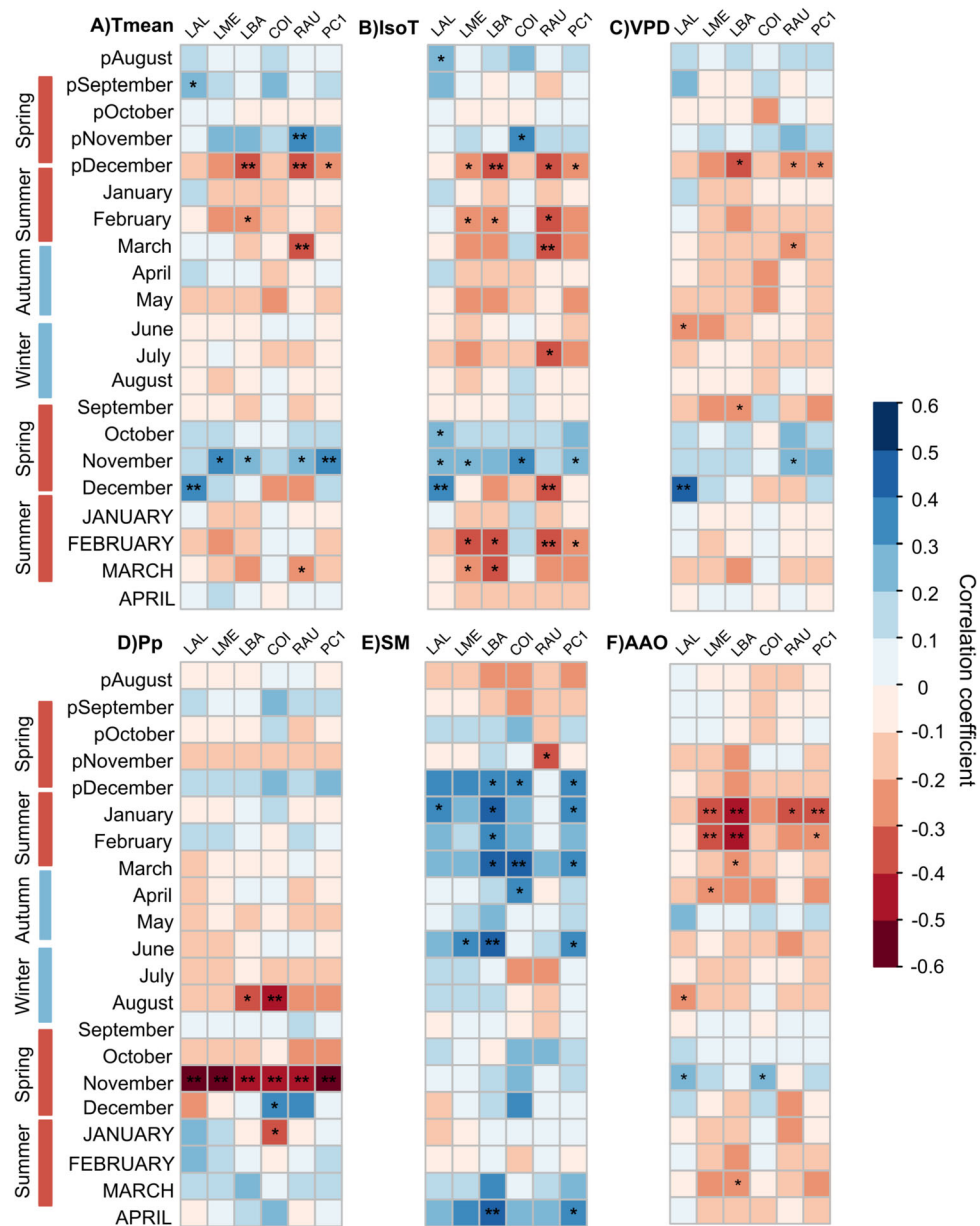


Figure 5. Pearson correlation coefficients between the standard chronologies of *Nothofagus pumilio* (LAL = high elevation; LME = mid-elevation; LBA = low elevation), *N. dombeyi* (COI); *N. alpina* (RAU), PC1, and monthly environmental variables at the Choshuenco volcano. The principal component analysis (PCA) was calculated from five *Nothofagus* species chronologies covering the period 1900–2019. **A** Mean temperature (Tmean; 1959–2019), **B** 0 °C Isotherm height (IsoT; 1958–2019), **C** Vapor pressure deficit (VPD; 1959–2019), **D** Precipitation CR2Met data (Pp; 1981–2019), **E** Soil moisture (SM; 1987–2019), and **F** Antarctic Oscillation Index (AAO). Correlation analyses were calculated from August of the previous growing season to April of the current growth season. Before performing the correlation analyses between the standard chronologies and environmental variables, the latter were detrended using an autoregressive model (* $p < 0.05$; ** $p < 0.01$).

The correlation field maps between the main mode (PC1) of *Nothofagus* forests tree growth and geopotential height and zonal wind gridded fields show a robust association between tree growth and large-scale tropospheric circulation conditions during the previous summer in the mid- to high-

latitudes of the Southern Hemisphere (Figure 6). The most notable features in the correlation maps indicate that the main mode of *Nothofagus* tree growth in our study area is strongly related to blocking activity and atmospheric circulation patterns in the extratropical southeastern Pacific.

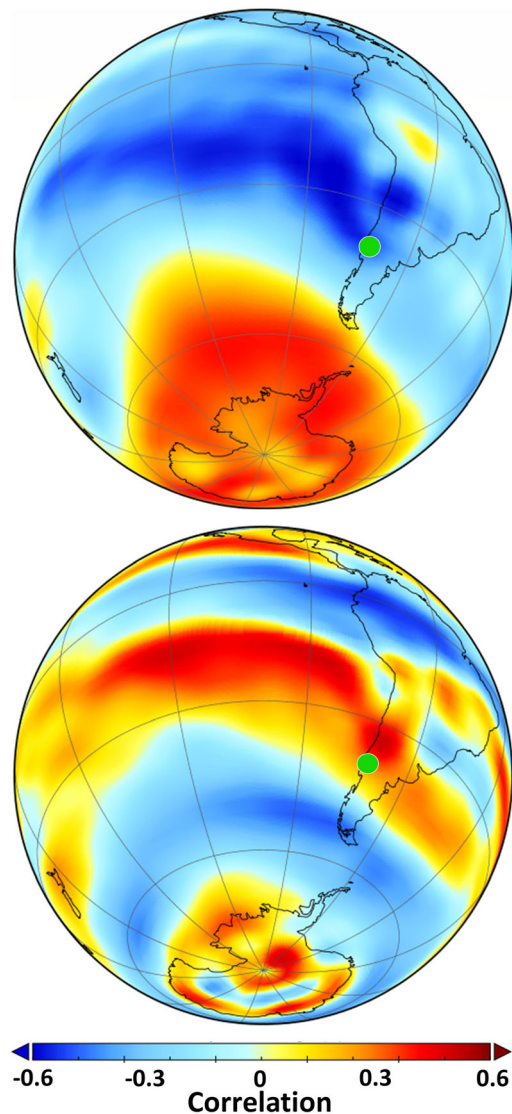


Figure 6. Spatial correlation fields between the *Nothofagus* PC1 growth patterns and previous Summer (Jan–Mar) $2.5^\circ \times 2.5^\circ$ 800mb Geopotential Height (up) and 600mb Zonal wind (bottom), respectively (period 1948–2019). The green dots indicate the location of the tree-ring sites in the windward side of the northern Patagonian Andes.

Resilience Indices in the *Nothofagus* Sites

Considering all four drought events together (1983, 1988, 1996, 1998), the radial growth resistance of trees in *N. pumilio* at high altitude and mid-altitude showed values below 1, while *N. pumilio* at low altitude and *N. dombeyi* showed an increasing trend, exceeding the value of 1. The highest and significantly different resistance value was found in *N. alpina*. For the recovery index, values slightly below and above 1 were recorded at the *N. pumilio*

high-, mid-, and low-altitude sites, while *N. dombeyi* showed a significantly lower value. In terms of resilience, the values were close to 1 at the *N. pumilio* high-, mid-, and low-altitude sites, while *N. dombeyi* showed the lowest and significantly different value, and *N. alpina* the highest (Figure 7).

Individual Growth Patterns and Resilience of Trees Grouped by PC1 Correlation

Approximately 75% of the series ($n = 376$) showed significant positive correlations with PC1 ($p < 0.05$), particularly in high- and mid altitude sites of *N. pumilio*. Mean ring-width series showed differences between correlated and non-correlated groups. In the series significantly correlated with PC1 tended to show a decrease in the mean ring width index, followed by a slight increase after 2010 that was not captured by regime shift analysis. Regarding drought response, trees positively correlated with PC1 exhibited significantly higher recovery and resilience values ($p < 0.05$) compared to non-correlated series.

DISCUSSION

Temporal Patterns of the Chronologies

The five *Nothofagus* chronologies of the three co-occurring species developed on the high-elevation forests of the Choshuenco volcano showed EPS values above 0.85 from 1870 to the present (Figure 2; Table 1), demonstrating adequate sample replication and a high common signal for tree growth at each site. Additionally, our chronologies showed inter-series correlations from 0.48 to 0.53 (Table 1) that are relatively high compared to previous chronologies of *N. pumilio*. For example, this species showed inter-series correlations between 0.12 and 0.38 in the northern part of its distribution on the western slope of the Andes (Lara and others 2001). The chronology of *N. dombeyi* showed a correlation value of 0.53 among the series, which is higher than the values reported by Suarez (2010), ranging from 0.39 to 0.47 in drier sites on the eastern side of the Andes. Additionally, the EPS of *N. dombeyi* was similar (> 0.85) to the values reported by Guzmán-Marín and others (2024). *N. alpina* showed an inter-series correlation of 0.48, similar to those reported by Bonada and others (2022a) at their sites on the eastern slope of the Andes, where mesic conditions prevail along an annual precipitation gradient ranging from 934 to 1461 mm at the wetter location. The high correla-

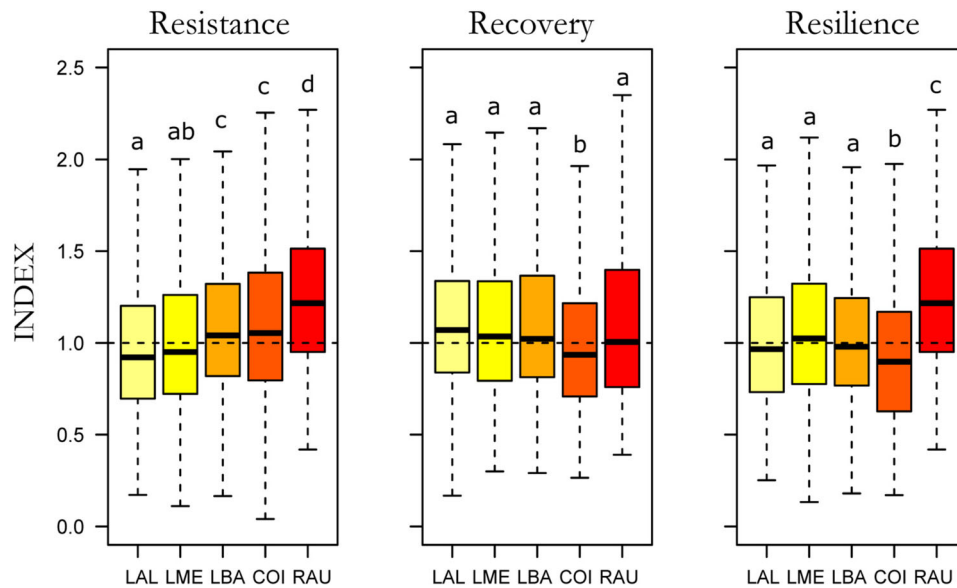


Figure 7. Resistance, recovery, and resilience indices of the chronologies along the altitudinal gradient. The indices are shown considering the events 1983, 1988, 1996 and 1998 recorded by Palmer Drought Severity Index (scPDSI; Figure S1). *Nothofagus pumilio* (LAL = high elevation; LME = mid-elevation; LBA = low elevation), *N. dombeyi* (COI) and *N. alpina* (RAU). The index values were calculated based on the positive correlation observed between radial growth and soil moisture during the previous growing season (Figure 5E). Consequently, the indices for the growing seasons following the drought years were computed to assess the drought resilience of the tree species. The boxes represent the 25th and 75th percentiles, with the central lines indicating the median. A Kruskal–Wallis test was performed followed by a Dunn post hoc test with Bonferroni adjustment. Letters indicate significant differences between sites ($p < 0.05$).

tion values among the series (Table 1) and between the medium- and low-altitude *N. pumilio* chronologies (Figure 3) support the findings of Villalba and others (1997), who observed stronger correlations in *N. pumilio* growing at mid-elevations compared to sites near the altitudinal treeline. The decreasing growth trend observed in *N. pumilio* chronologies at high, medium, and low altitudes is also evident in *N. dombeyi* (1990–2015) and *N. alpina* (1990–2010). These declining growth trends in recent decades have been previously reported in conifers from central-southern Chile, such as *Austrocedrus chilensis*, *Araucaria araucana* (Villalba and others 2012), and *Prumnopitys andina* (Álvarez and others 2021). A similar declining trend has also been observed in the angiosperms *N. dombeyi* on both slopes of the Andes (Guzmán-Marín and others 2024; Suarez and others 2004) and *N. pumilio*, with cases of individual tree mortality on the eastern slopes of the Andes (Rodríguez-Catón and others 2016; Suarez and others 2004). Over the past 120 years, significant positive correlations have been observed between chronologies of different species, such as between *N. pumilio* medium altitude and *N. alpina*, and, *N. pumilio* low altitude and *N. alpina* ($p < 0.05$; Figure 3). These strong correlations suggest that a common environmental

factor may be responsible for this high synchronicity across species. The increase in the percentage of variance explained by PC1 in the five *Nothofagus* chronologies analyzed indicates greater synchrony in tree growth after 1980 (Figure 4), suggesting an increased common signal affecting radial tree growth. This indicates that the growth curves of the chronologies have become more aligned, suggesting that the limiting factor may be the same for all sites and species and may be intensified over time in mountainous areas of the Andes. The increased common signal in tree radial growth may be related to climatic variables shifts that occurred during the 1970s. Changes in precipitation, as well as in minimum and maximum temperature regimes, have been detected in the study area around 40°S (Figures S2–S4). This is consistent with observations reported for South-Central Chile during 1976–1977 (Jacques-Coper and Garreaud 2015).

This trend of increasing common signal after 1980 can also be observed at the chronology level, with a slight rise in the variance explained by PC1 in *N. pumilio* high and low altitude, and *N. dombeyi*. The results for *N. pumilio* low altitude align with previous findings for the site, where analysis showed a decline in PC1 at the end of the 1980 s,

leading to a decrease in the common signal influencing tree growth at this location. Serrano-León and Christie (2020) attributed this loss of common signal to anomalous growth patterns caused by partial canopy dieback in individual trees. However, our results indicate an increase in the variance explained by PC1, and consequently, a subsequent rise in the common signal after the earlier decline. This suggests a recovery of the common growth pattern and the possible survival of trees that experienced canopy damage during that period. The return to more stable growth in recent years in *N. pumilio* low altitude is also evident in the growth curve of its chronology (Figure 2C).

Relationship Between Radial Growth and Environmental Variables

The most notable pattern observed in the correlations between environmental variables and the growth of the analyzed tree species was the strong negative relationship between November precipitation during the current growing season and all five chronologies, as well as PC1. Additionally, there is a positive relationship between radial growth and both Tmean as well as IsoT °C in most sites (Figure 5A, B). Specifically, the positive correlation with mean temperature in November (Tmean) suggests that snow cover at the beginning of the growing season has become increasingly more limiting (Figure 5A). This response is linked to the type of precipitation that occurs during this particular month. When precipitation occurs at lower temperatures, snow can accumulate and remain on the soil, delaying the onset of the growing season and shortening its duration, which leads to the formation of narrower tree rings on the studied species (Villalba and others 2003). These findings in *N. pumilio* are consistent with previous reported by Álvarez and others (2015) and Serrano-León and Christie (2020) for the sites *N. pumilio* high and low altitude, as well as with the results found by Villalba and others (1997) and Lavergne and others (2015) on the eastern slope of the Andes.

It has been reported that *N. pumilio* responds specifically to climatic variability along its latitudinal distribution gradient. In the norther part of its range (36°S–39°S), a significant positive relationship with precipitation and a negative relationship with temperature have been observed (Lara and others 2005). In this study conducted near 40°S, we found that although *N. pumilio* is in the northern sector of its latitudinal distribution, there was a significant negative relationship between radial

growth and precipitation, and a significant positive relationship with temperature at the beginning of the current growing season. Therefore, both precipitation and temperature were important for the radial growth of the species. This finding is consistent with radial growth increases when the 0 °C isotherm height rises, indicating that growth of *N. pumilio* improves when snowfall occurs at higher elevations (Figure 5B). Similarly, soil moisture (SM) was found to be important for *N. pumilio* during the summer of the previous growing season, particularly for *N. pumilio* low-altitude site, which exhibited positive correlations between radial growth and soil moisture from December to March (Figure 5E).

The *N. dombeyi* individuals sampled in this study are located near its altitudinal limit and in the central part of the latitudinal range of the species, where climatic conditions are nearly optimal for growth. Additionally, the site is characterized by deep soils and abundant water availability (Donoso 1974). Therefore, the negative relationship observed between radial growth of *N. dombeyi* and precipitation during winter (that is, August) and at the beginning of the growing season (i.e., November) was unexpected. This could be related to the evergreen nature of the species, as abundant precipitation in winter and early spring can damage the tree canopy, reducing its photosynthetic capacity and ultimately limiting growth. This result contrasts with those reported by Guzmán-Marín and others (2024), who found positive correlations between the radial growth of *N. dombeyi* and summer precipitation, as well as negative correlations with maximum temperature, at the San Pablo site, located approximately 30 km north of our study area. Similar to *N. pumilio*, soil moisture showed significant positive correlations with *N. dombeyi* growth during the previous growing season, emphasizing the importance of water availability for growth during the summer.

For *N. alpina*, we studied a population located near the southern limit of its latitudinal distribution, where higher sensitivity to limiting climatic variables is expected. The results support this expectation, showing a negative correlation between growth and precipitation, and a positive correlation with mean November temperature, consistent with the other species studied. These findings contrast with those reported by Bonada and others (2022b), likely due to the greater water availability at the Choshuenco volcano compared to the climate characterized by a pronounced summer drought on the eastern slope of the Andes. Furthermore, significant shifts in the correlations

between growth and mean temperature are observed on a monthly scale within the same growing season. Specifically, the correlation changes from positive in November to significantly negative in December and March of the previous growing season (Figure 5A). This is consistent with mean sensitivity values around 0.31, which may indicate a high sensitivity of tree growth to climate variability. These mean sensitivity values are higher than those reported for other species, such as *Austrocedrus chilensis* (0.11–0.22; Amoroso and others 2012), *Araucaria araucana* (0.14–0.23; Muñoz and others 2014), and *Prumnopitys andina* (mean sensitivity of 0.27; Álvarez and others 2021). In contrast to the responses observed in the other *Nothofagus* species analyzed, *N. alpina* does not exhibit positive correlations with soil moisture during the previous summer. This suggests that soil water availability is not a limiting factor for tree radial growth, this may be associated with geographic location of our study area, which is situated near the southern limit of its latitudinal range.

Finally, the negative correlation between the AAO and tree growth during the summer months of the previous growing season indicates that positive AAO conditions (i.e., high pressures in mid-latitudes) lead to below-average growth of the main pattern of tree growth represented by PC1 (Figure 5F). This would be due the observed reduction in summer precipitation in the study area when the AAO is in its positive phase (González-Reyes and Muñoz 2013; Álvarez and others 2015). The previous is consistent with the large-scale circulation patterns depicted by the correlation maps (Figure 6). These maps indicate that low values of the main mode of tree growth (PC1) are associated with high and low geopotential height anomalies over mid-latitudes and Antarctica, respectively. These pressure patterns drive the southward migration of the westerly storm track, resulting in anomalously warm and dry summer conditions in our study region (Gillett and others 2006; Garreaud and others 2009; Christie and others 2011; Morales and others 2020). These large-scale climate patterns are coincident with the positive phase of the AAO, corroborating the influence of this forcing over the hydroclimate of northern Patagonia and thus tree growth.

Growth Responses to Drought

As expected, the results for the drought resistance (R_t), recovery (R_c), and resilience (R_s) indices show a variable growth response across the altitudinal gradient and in relation to drought occur-

rence (Figure 7; Fang and Zhang 2019; Su and others 2021). Overall, these values remain within a narrow range, close to 1, consistent with values observed in *N. obliqua* forests along a latitudinal gradient in south-central Chile (Urrutia-Jalabert and others 2021).

In the case of *N. pumilio*, the resistance and recovery indices showed values slightly below and above 1, respectively, with higher values observed at the *N. pumilio* low altitude site. Resilience, which measures the ability of trees to recover their pre-drought growth, remained close to 1 (Figure 7), indicating that growth rates before and after drought events were not significantly affected by dry conditions. The relatively minor impact of drought on *N. pumilio* may be attributed to the extremely wet conditions that prevail during the fall and winter, which likely may mitigate the negative effects of drought during growing season.

N. dombeyi showed moderate resistance to drought ($R_t > 1$), but low recovery ($R_c < 1$) and slight low resilience ($R_s < 1$), suggesting that, although this species can resist drought events relatively well, it struggles to recover its growth once conditions improve. This may be attributed to the preference of *N. dombeyi* for humid environments, where its recovery capacity tends to be higher. In more xeric sites, such as those on the eastern slope of the Andes, the species is more severely affected by droughts, showing resistance below 1 ($R_t < 1$), recovery above 1 ($R_c > 1$), and slightly higher resilience ($R_s > 1$; Suarez and others 2024). These contrasting responses highlight the significant influence of local environmental conditions on the drought dynamics of *N. dombeyi*.

N. alpina showed high values in resistance (R_t), recovery (R_c), and resilience (R_s) indices, (Figure 7), indicating that the species is well-adapted to drought conditions and recovers effectively after dry periods. These findings suggest that *N. alpina* growing in our study area maintains and restores its growth even under dry conditions. The high resilience of this species may be attributed to its location near the southern limit of its latitudinal range, where dry conditions may actually create a favorable environment for its growth (Figure 5). Consequently, trees of this species exhibit adaptability and stability despite variations in water availability.

Growth Response and Resilience at the Individual Tree Level

An important finding from this tree-level analysis was the high proportion of series that correlated

with PC1, indicating strong coherence in tree responses, particularly *N. pumilio*, to climatic variability (Figure 8). This finding supports the validity of PC1, derived from the chronology-level analysis (Figure 2F), as a representative time series of common growth signal in the study area, likely reflecting a dominant regional climate influence. In

the case of *N. alpina*, the smaller number of samples collected compared to *N. dombeyi* and *N. pumilio* suggests that its results should be interpreted with caution. The mean growth curve of the series correlated with PC1 shows a notable decline in radial growth in recent decades (Figure 8A), which may be linked to a slight increase in precipitation and a

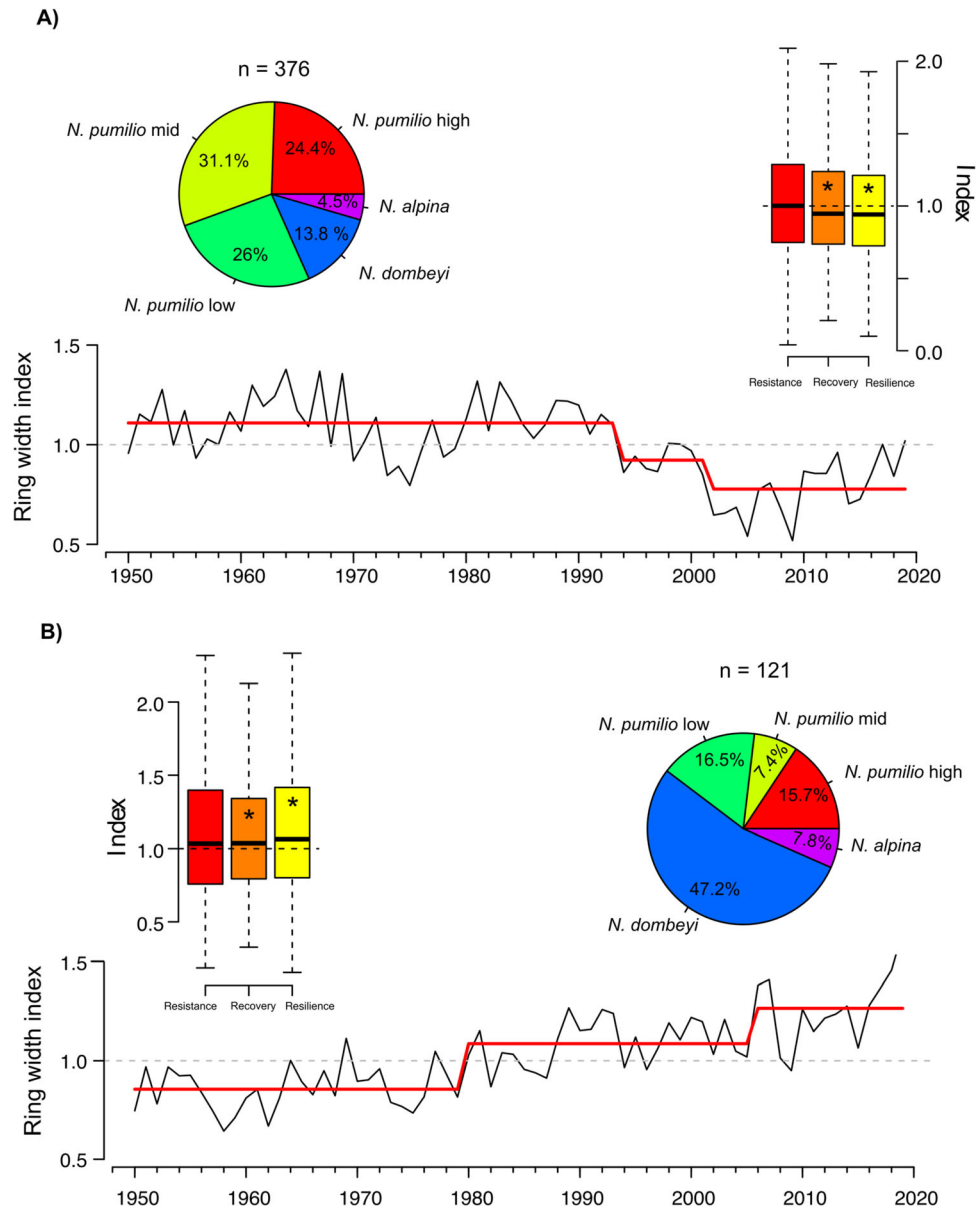


Figure 8. **A** *Nothofagus* multispecies tree-ring series from Choshuenco volcano significantly correlated with the PC1 amplitude series at the 95% of confidence level. **B** *Nothofagus* multispecies tree-ring series from Choshuenco volcano non-significantly correlated with the PC1 amplitude. In both panels, the mean ring width index is shown. The red lines indicate regime shifts detected using the Rodionov (2004) method (window length = 10 years, 95% c.l.). Resistance, recovery, and resilience indices were calculated for both groups, and differences were assessed using the non-parametric Mann–Whitney U test. Asterisks indicate statistically significant differences ($p < 0.05$) between indices of both groups. The pie charts on each panel represents the relative percentage of individuals of each *Nothofagus* species contributing to each multispecies tree-ring chronologies (n = total number of tree individuals on each chronology).

decrease in spring temperatures specifically in November, a key month for growth in the studied species (Álvarez and others 2015; Serrano-León and Christie 2020; Figure 5). This pattern is consistent with the moving correlation analyses, which identify November temperature, precipitation, and the Palmer Drought Severity Index (PDSI) as the main climatic drivers (Figures S5–S8). As expected, trees that experienced a decline in ring-width indices in recent decades also exhibited significantly lower values of recovery and resilience compared to those showing an increase trend in growth (Figure 8A).

The findings obtained through the individual series approach generally confirm the results previously observed using ring-width chronologies. A decline in growth beginning in the 1990s, followed by an increase after 2010, is highlighted and associated primarily with November temperature and precipitation conditions. Higher precipitation combined with lower temperatures during this critical spring month likely results in a shortened growing season, leading to reduced cambial activity and the formation of narrower tree rings under such conditions (Figure 5).

CONCLUSIONS

The analysis of radial growth patterns of three co-occurring *Nothofagus* species across the altitudinal gradient of the Choshuenco volcano in the Valdivian Andes reveals strong growth synchrony high inter-series correlations. Recent growth declines are consistent with regional trends in the northern Patagonian Andean forests, suggesting increased climatic stress. A rising common growth signal after 1980 suggests intensifying environmental drivers linked to climate variability.

The relationship between radial growth and environmental variables shows distinct species-specific responses influenced by altitudinal and climatic factors. All species exhibited a negative correlation with precipitation at the beginning of the growing season (November), with some also showing a positive correlation with mean November temperature and the 0 °C isotherm height, highlighting the significant impact of early growing season conditions on growth. Snow accumulation, which delays the onset of growth, emerges as a key limiting factor for *N. pumilio*, while soil moisture during previous summer plays an important role at most species sites. The growth responses to drought vary among species influenced by local conditions. *N. pumilio* showed minimal drought impact, likely due to wet conditions during fall and winter. *N.*

dombeyi exhibited moderate resistance but struggled to restore its growth to pre-drought conditions. *N. alpina* showed high resistance, recovery and resilience, suggesting drought adaptation potentially due to its location at the southern edge of its species range. The individual tree-ring analysis at tree level demonstrated that a large number of tree-ring series present significant correlations with dominant growth pattern (PCI) reflecting a high degree of coherence in growth responses to climate variability.

These findings highlight the complex interplay between environmental variables and species-specific and individual-level growth responses, emphasizing the relevance of climatic factors in responses of *Nothofagus* species to changing environmental conditions in the Valdivian Andes of northern Patagonia.

ACKNOWLEDGEMENTS

This research was funded by the Chilean Research Council (ANID) Grants: FONDECYT 1241699, FONDAF/1523A0002, ANID/BASALFB210018. C.A. acknowledges financial support from ANID PFCHA/Doctorado Nacional/2018-21181009, a postdoctoral fellowship from the Cape Horn International Center (CHIC, ANID/BASAL FB210018), and a postdoctoral fellowship from ANID FONDECYT/Postdoctorado/2025-3250612.

DATA AVAILABILITY

Data for this study can be found in the Supplemental Information associated with the paper.

REFERENCES

- Aceituno P. 1988. On the functioning of the southern oscillation in the South America, sector. Part I: Surface Climate, 1988. Monthly Water Review 116:505–524.
- Álvarez C, Veblen TT, Christie DA, González-Reyes Á. 2015. Relationships between climate variability and radial growth of *Nothofagus pumilio* near altitudinal treeline in the Andes of northern Patagonia, Chile. For Ecol Manag 342:112–121. <https://doi.org/10.1016/j.foreco.2015.01.018>.
- Álvarez C, Le Quesne C, Rojas-Badilla M, Rozas V, González-Reyes Á. 2021. Dendrochronological potential of *Prumnopitys andina* (Podocarpaceae) at the southern limit of its range in the Chilean Andes. N Z J Bot 59:423–439. <https://doi.org/10.1080/0028825x.2021.1877158>.
- Amoroso MM, Daniels LD, Larson BC. 2012. Temporal patterns of radial growth in declining *Austrocedrus chilensis* forests in Northern Patagonia: The use of tree-rings as an indicator of forest decline. For Ecol Manage 265:62–70. <https://doi.org/10.1016/j.foreco.2011.10.021>.
- Arias PA, Bellouin N, Coppola E, Jones RG, Krinner G, Marotzke J, Naik V, Palmer MD, Plattner G-K, Rogelj J, Rojas M, n.d. 2021. Technical Summary. In Climate Change 2021: The

- Physical Science Basis. Contribution of Working Group I to the Sixth Assessment Report of the Intergovernmental Panel on Climate Change. Cambridge University Press, Cambridge, United Kingdom; New York, NY, USA.
- Barichivich J, Osborn TJ, Harris I, Schrier G, Jones PD, Aldred F, Gobron N, Miller JB, Willett KM. 2021. Monitoring global drought using the self-calibrating Palmer Drought Severity Index. *Bulletin of the American Meteorological Society* 102.
- Bonada A, Amoroso M, Gedalof Z. 2022a. The First Network of Tree-Ring Chronologies for Co-Occurring *Nothofagus nervosa* and *Nothofagus obliqua* along a Precipitation Gradient in Patagonia, Argentina. *Tree Ring Res* 78. <https://doi.org/10.3959/trr2021-8>
- Bonada A, Amoroso MM, Gedalof Z, Srur AM, Gallo L. 2022b. Effects of climate on the radial growth of mixed stands of *Nothofagus nervosa* and *Nothofagus obliqua* along a precipitation gradient in Patagonia, Argentina. *Dendrochronologia* (Verona) 74:125961. <https://doi.org/10.1016/j.dendro.2022.125961>.
- Burschel P, Gallegos C, Martínez O, Moll W. 1976. Composición y dinámica regenerativa de un bosque virgen mixto de raulí y coigüe. *Bosque*. 2:55–74.
- Caldcleugh A. 1836. An Account of the great earthquake experienced in Chile on the 20th of February, 1835: with a map. *Philos Trans R Soc Lond* 126:21–26.
- Cook ER, Holmes RL. 1984. Program ARSTAN User Manual, Laboratory of Tree Ring Research. Tucson
- Cook ER, Briffa K, Shiyatov S, Mazepa V. 1990. Tree ring standardization and growth-trend estimation. In: Cook E, Kairiuktis L, Eds. *Methods of Dendrochronology*. Dordrecht: Kluwer Academic Publishers. pp 104–132.
- Christie DA, Boninsegna JA, Cleaveland MK, Lara A, Le Quesne C, Morales MS, Mudelsee M, Stahle DW, Villalba R. 2011. Aridity changes in the Temperate-Mediterranean transition of the Andes since ad 1346 reconstructed from tree-rings. *Clim Dyn* 36:1505–1521. <https://doi.org/10.1007/s00382-009-0723-4>.
- Daniels LD, Veblen TT. 2003. Regional and local effects of disturbance and climate on altitudinal treelines in northern Patagonia. *J Veg Sci* 14:733–742. <https://doi.org/10.1111/j.1654-1103.2003.tb02205.x>.
- Daniels LD, Veblen TT. 2004. Spatiotemporal influences of climate on altitudinal treeline in northern Patagonia. *Ecology* 85:1284–1296. <https://doi.org/10.1890/03-0092>.
- Donoso C. 1974. *Dendrología: Árboles y Arbustos Chilenos*. Universidad de Chile, Facultad de Ciencias Forestales. 142.
- Donoso C, Deus R, Cockbaine JC, Castillo H. 1986. Variaciones estructurales del tipo forestal Coihue-Raulí-Tepa. *Bosque* 7:17–35.
- Donoso C. 1993. *Ecología Forestal: el bosque y su medio ambiente*. Santiago: Editorial Universitaria.
- Fang O, Zhang Q-B. 2019. Tree resilience to drought increases in the Tibetan Plateau. *Glob Chang Biol* 25:245–253. <https://doi.org/10.1111/gcb.14470>.
- Fritts HC. 1976. *Tree Rings and Climate*. London: Academic Press. p 567.
- Fyfe JC. 2003. Separating extratropical zonal wind variability and mean change. *J Clim* 16:863–874. [https://doi.org/10.1175/1520-0442\(2003\)016%3c0863:sezwwa%3e2.0.co;2](https://doi.org/10.1175/1520-0442(2003)016%3c0863:sezwwa%3e2.0.co;2).
- Garreaud RD, Vuille M, Compagnucci R, Marengo J. 2009. Present-day south American climate. *Palaeogeogr Palaeoclimatol Palaeoecol* 281:180–195. <https://doi.org/10.1016/j.palaeo.2007.10.032>.
- Garreaud RD, Alvarez-Garreton C, Barichivich J, Boisier JP, Christie D, Galleguillos M, LeQuesne C, McPhee J, Zambrano-Bigiarini M. 2017. The 2010–2015 megadrought in central Chile: impacts on regional hydroclimate and vegetation. *Hydrol Earth Syst Sci* 21:6307–6327. <https://doi.org/10.5194/hess-21-6307-2017>.
- Gazol A, Camarero JJ, Anderegg WRL, Vicente-Serrano SM. 2017. Impacts of droughts on the growth resilience of Northern Hemisphere forests: Forest growth resilience to drought. *Glob Ecol Biogeogr* 26:166–176. <https://doi.org/10.1111/geb.12526>.
- Gillett NP, Kell TD, Jones PD. 2006. Regional climate impacts of the Southern Annular Mode. *Geophys Res Lett*. <https://doi.org/10.1029/2006gl027721>.
- González-Reyes Á, Muñoz AA. 2013. Cambios en la precipitación de la ciudad de Valdivia (Chile) durante los últimos 150 años. *Bosque (Valdivia)* 34:191–200. <https://doi.org/10.4067/s0717-92002013000200008x>.
- González-Reyes Á, Jacques-Coper M, Muñoz AA. 2020. Seasonal precipitation in South Central Chile: trends in extreme events since 1900. *Atmósfera*. <https://doi.org/10.20937/atm.52871>
- González-Reyes Á, Jacques-Coper M, Bravo C, Rojas M, Garreaud R. 2023. Evolution of heatwaves in Chile since 1980. *Weather Clim Extrem* 41:100588. <https://doi.org/10.1016/j.wace.2023.100588>.
- Gormaz V. 1869. *Continuación de los trabajos de exploración del Río Valdivia I sus afluentes*. Chile: Imprenta Nacional.
- Guzmán-Marín R, He M, Rossi S, Rodríguez CG, Urrutia-Jalabert R, Lara A. 2024. Growth decline and wood anatomical traits in *Nothofagus dombeyi* populations along a latitudinal gradient in the Andes. *Chile Trees (Berl West)*. <https://doi.org/10.1007/s00468-024-02564-z>.
- Harris I, Osborn TJ, Jones P, Lister D. 2020. Version 4 of the CRU TS monthly high-resolution gridded multivariate climate dataset. *Sci Data* 7:109. <https://doi.org/10.1038/s41597-020-0453-3>.
- Hartmann, DL. 2016. Symbol definitions. In: *Global Physical Climatology*. Elsevier. pp 431–442. <https://doi.org/10.1016/C2009-0-00030-0>
- Hersbach H, Bell B, Berrisford P, Hirahara S, Horányi A, Muñoz-Sabater J, Nicolas J, Peubey C, Radu R, Schepers D, Simmons A, Soci C, Abdalla S, Abellan X, Balsamo G, Bechtold P, Bivattini G, Bidlot J, Bonavita M, De Chiara G, Dahlgren P, Dee D, Diamantakis M, Dragani R, Flemming J, Forbes R, Fuentes M, Geer A, Haimberger L, Healy S, Hogan RJ, Hólm E, Janisková M, Keeley S, Laloyaux P, Lopez P, Lupu C, Radnoti G, de Rosnay P, Rozum I, Vamborg F, Villaume S, Thépaut Jean-Noël. 2020. The ERA5 global reanalysis. *Q J R Meteorol Soc* 146:1999–2049. <https://doi.org/10.1002/qj.3803>.
- Hildebrand-Vogel R, Godoy R, Vogel A. 1990. Subantarctic-Andean *Nothofagus pumilio* forests: Distribution area and synsystematic overview; vegetation and soils as demonstrated by an example of a South Chilean stand. *Vegetatio* 89:55–68. <https://doi.org/10.1007/bf00134434>.
- Holmes RL. 1983. Computer-assisted quality control in tree-ring dating and measurement. *Tree-Ring Bulletin* 44:69–75.
- Jacques-Coper M, Garreaud RD. 2015. Characterization of the 1970s climate shift in South America. *Int J Climatol* 35:2164–2179. <https://doi.org/10.1002/joc.4120>.

- Kistler R, Collins W, Saha S, White G, Woollen J, Kalnay E, Chelliah M, Ebisuzaki W, Kanamitsu M, Kousky V, van den Dool H, Jenne R, Fiorino M. 2001. The NCEP–NCAR 50–year reanalysis: Monthly means CD–ROM and documentation. *Bull Am Meteorol Soc* 82:247–267. [https://doi.org/10.1175/1520-0477\(2001\)082%3c0247:tynyrm%3e2.3.co;2](https://doi.org/10.1175/1520-0477(2001)082%3c0247:tynyrm%3e2.3.co;2).
- Lara A, Aravena JC, Villalba R, Wolodarsky-Franke A, Luckman B, Wilson R. 2001. Dendroclimatology of high-elevation *Nothofagus pumilio* forests at their northern distribution limit in the central Andes of Chile. *Can J for Res* 31:925–936. <https://doi.org/10.1139/cjfr-31-6-925>.
- Lara A, Villalba R, Wolodarsky-Franke A, Aravena JC, Luckman BH, Cuq E. 2005. Spatial and temporal variation in *Nothofagus pumilio* growth at tree line along its latitudinal range (35°–55° S) in the Chilean Andes. *Journal of Biogeography*:879–93.
- Lavergne A, Daux V, Villalba R, Barichivich J. 2015. Temporal changes in climatic limitation of tree-growth at upper treeline forests: Contrasted responses along the west-to-east humidity gradient in Northern Patagonia. *Dendrochronologia* (Verona) 36:49–59. <https://doi.org/10.1016/j.dendro.2015.09.001>.
- Lloret F, Keeling EG, Sala A. 2011. Components of tree resilience: effects of successive low-growth episodes in old ponderosa pine forests. *Oikos* 120:1909–1920. <https://doi.org/10.1111/j.1600-0706.2011.19372.x>.
- Marshall GJ. 2003. Trends in the southern annular mode from observations and reanalyses. *J Clim* 16:4134–4143. [https://doi.org/10.1175/1520-0442\(2003\)016%3c4134:titsam%3e2.0.co;2](https://doi.org/10.1175/1520-0442(2003)016%3c4134:titsam%3e2.0.co;2).
- Martens B, Miralles DG, Lievens H, van der Schalie R, de Jeu RAM, Fernández-Prieto D, Beck HE, Dorigo WA, Verhoest NEC. 2017. GLEAM v3: satellite-based land evaporation and root-zone soil moisture. *Geosci Model Dev* 10:1903–1925. <https://doi.org/10.5194/gmd-10-1903-2017>.
- McNally A, Arsenault K, Kumar S, Shukla S, Peterson P, Wang S, Funk C, Peters-Lidard CD, Verdin JP. 2017. A land data assimilation system for sub-Saharan Africa food and water security applications. *Sci Data* 4:170012. <https://doi.org/10.1038/sdata.2017.12>.
- Minder JR, Durran DR, Roe GH. 2011. Mesoscale controls on the mountainside snow line. *J Atmos Sci* 68:2107–2127. <https://doi.org/10.1175/jas-d-10-05006.1>.
- Morales MS, Cook ER, Barichivich J, Christie DA, Villalba R, LeQuesne C, Srur AM, Ferrero ME, González-Reyes Á, Couvreur F, Matskovsky V, Aravena JC, Lara A, Mundo IA, Rojas F, Prieto MR, Smerdon JE, Bianchi LO, Masiokas MH, Urrutia-Jalabert R, Rodríguez-Catón M, Muñoz AA, Rojas-Badilla M, Alvarez C, Lopez L, Luckman BH, Lister D, Harris I, Jones PD, Williams AP, Velazquez G, Aliste D, Aguilera-Betti I, Marcotti E, Flores F, Muñoz T, Cuq E, Boninsegna JA. 2020. Six hundred years of South American tree rings reveal an increase in severe hydroclimatic events since mid-20th century. *Proc Natl Acad Sci U S A* 117:16816–16823. <https://doi.org/10.1073/pnas.2002411117>.
- Muñoz AA, Barichivich J, Christie DA, Dorigo W, Sauchyn D, González-Reyes Á, Villalba R, Lara A, Riquelme N, González ME. 2014. Patterns and drivers of *Araucaria araucana* forest growth along a biophysical gradient in the northern Patagonian Andes: Linking tree rings with satellite observations of soil moisture: Patterns and drivers of *Araucaria* growth. *Austral Ecol* 39:158–169. <https://doi.org/10.1111/aec.12054>.
- Pierce D. 2024. `_ncdf4`: Interface to Unidata netCDF (Version 4 or Earlier) Format Data Files_ R package version 1.2.3, <https://CRAN.R-project.org/package=ncdf4>.
- Rebertus A, Veblen TT. 1993. Structure and tree-fall gap dynamics of old-growth *Nothofagus* forests in Tierra del Fuego, Argentina. *Journal of Vegetation Science* 4:641–654.
- Rodionov SN. 2004. A sequential algorithm for testing climate regime shifts. *Geophys Res Lett*. <https://doi.org/10.1029/2004gl019448>.
- Rodríguez-Catón M, Villalba R, Morales M, Srur A. 2016. Influence of droughts on *Nothofagus pumilio* forest decline across northern Patagonia, Argentina. *Ecosphere* 7. <https://doi.org/10.1002/ecs2.1390>
- Rojas-Badilla M, LeQuesne C, Rozas V, Gipoulou-Zúñiga T, González-Reyes Á, Copenheaver CA. 2023. Species-specific influence of hydroclimate on secondary growth of three coexisting conifers in a temperate Andean forest in south-central Chile. *Dendrochronologia* (Verona) 80:126113. <https://doi.org/10.1016/j.dendro.2023.126113>.
- Schulman E. 1956. *Dendroclimatic Changes in Semiarid America*. Tucson: University Arizona Press.
- Seidl R, Thom D, Kautz M, Martin-Benito D, Peltoniemi M, Vacchiano G, Wild J, Ascoli D, Petr M, Honkaniemi J, Lexer MJ, Trotsiuk V, Mairota P, Svoboda M, Fabrika M, Nagel TA, Reyer CPO. 2017. Forest disturbances under climate change. *Nat Clim Chang* 7:395–402. <https://doi.org/10.1038/nclimate3303>.
- Serrano-León H, Christie DA. 2020. Tree-growth at the rear edge of a *Nothofagus pumilio* Andean forest from Northern Patagonia show different patterns and a decline in the common signal during the last century. *For Ecol Manage* 475:118426. <https://doi.org/10.1016/j.foreco.2020.118426>.
- Srur AM, Villalba R, Villagra PE, Hertel D. 2008. Influencias de las variaciones en el clima y en la concentración de CO₂ sobre el crecimiento de *Nothofagus pumilio* en la Patagonia. *Rev Chil Hist Nat* 81. <https://doi.org/10.4067/s0716-078x200800200007>
- Su J, Shen J, Li S, Huang X, Liu W, Lang X. 2021. Quantifying radial growth response of *Pinus yunnanensis* to climate change and drought event at different altitudes and ages in the Jinsha River Basin. *Research Square*. <https://doi.org/10.21203/rs.3.rs-633818/v1>
- Suarez ML. 2010. Tree-ring records from *Nothofagus dombeyi*: A preliminary chronology network in Northern Patagonia, Argentina. *Dendrochronologia* (Verona) 28:65–72. <https://doi.org/10.1016/j.dendro.2009.11.001>.
- Suarez ML, Ghermandi L, Kitzberger T. 2004. Factors predisposing episodic drought-induced tree mortality in *Nothofagus*-site, climatic sensitivity and growth trends. *J Ecol* 92:954–966. <https://doi.org/10.1111/j.1365-2745.2004.00941.x>.
- Suarez ML, Villalba R, Mundo IA, Schroeder N. 2015. Sensitivity of *Nothofagus dombeyi* tree growth to climate changes along a precipitation gradient in northern Patagonia, Argentina. *Trees* (Berl West) 29:1053–1067. <https://doi.org/10.1007/s00468-015-1184-5>.
- Suarez ML, Sasal Y, Facciano L. 2024. Factors driving unexpected drought-induced *Nothofagus dombeyi* mortality in a Valdivian temperate Rainforest, Argentina. *Forests* 15:1355. <https://doi.org/10.3390/f15081355>.
- Thompson DWJ, Wallace JM. 2000. Annular modes in the extratropical circulation. Part I: Month-to-Month Variability. *J Clim* 13:1000–1016. [https://doi.org/10.1175/1520-0442\(2000\)013%3c1000:amitec%3e2.0.co;2](https://doi.org/10.1175/1520-0442(2000)013%3c1000:amitec%3e2.0.co;2).
- Trenberth KE, Dai A, van der Schrier G, Jones PD, Barichivich J, Briffa KR, Sheffield J. 2014. Global warming and changes in

- drought. *Nat Clim Change* 4:17–22. <https://doi.org/10.1038/nclimate2067>.
- Treydte K, Boda S, Graf Pannatier E, Fonti P, Frank D, Ullrich B, Saurer M, Siegwolf R, Battipaglia G, Werner W, Gessler A. 2014. Seasonal transfer of oxygen isotopes from precipitation and soil to the tree ring: source water versus needle water enrichment. *New Phytol* 202:772–783. <https://doi.org/10.1111/nph.12741>.
- Urrutia-Jalabert R, Barichivich J, Rozas V, Lara A, Rojas Y, Bahamondez C, Rojas-Badilla M, Gipoulou-Zuñiga T, Cuq E. 2021. Climate response and drought resilience of *Nothofagus obliqua* secondary forests across a latitudinal gradient in south-central Chile. *For Ecol Manag* 485:118962. <https://doi.org/10.1016/j.foreco.2021.118962>.
- van der Maaten-Theunissen M, van der Maaten E, Bouriaud O. 2015. pointRes: An R package to analyze pointer years and components of resilience. *Dendrochronologia* (Verona) 35:34–38. <https://doi.org/10.1016/j.dendro.2015.05.006>.
- Veblen TT, Donoso C, Kitzberger T, Rebertus A, Veblen TT, Hill R, Reid J. 1996. Ecology of Southern Chilean and Argentinean *Nothofagus* Forests. 293–353.
- Venegas-González A, Gibson-Capintero S, Anholetto-Junior C, Mathiasen P, Premoli AC, Fresia P. 2022. Tree-ring analysis and genetic associations help to understand drought sensitivity in the Chilean endemic forest of *Nothofagus macrocarpa*. *Front For Glob Chang* 5. <https://doi.org/10.3389/ffgc.2022.762347>
- Villalba R, Boninsegna J, Veblen TT, Schmelter A, Rubulis S. 1997. Recent trends in Tree-rings Records from High Elevation Sites in the Andes of Northern Patagonia. *Climatic Change* 36:425–454.
- Villalba R, Lara A, Boninsegna JA, Masiokas M, Delgado S, Aravena JC, Roig FA, Schmelter A, Wolodarsky A, Ripalta A. 2003. *Clim Change* 59:177–232. <https://doi.org/10.1023/a:1024452701153>.
- Villalba R, Lara A, Masiokas MH, Urrutia R, Luckman BH, Marshall GJ, Mundo IA, Christie DA, Cook ER, Neukom R, Allen K, Fenwick P, Boninsegna JA, Srur AM, Morales MS, Araneo D, Palmer JG, Cuq E, Aravena JC, Holz A, LeQuesne C. 2012. Unusual Southern Hemisphere tree growth patterns induced by changes in the Southern Annular Mode. *Nat Geosci* 5:793–798. <https://doi.org/10.1038/ngeo1613>.
- Wells N, Goddard S, Hayes MJ. 2004. A self-calibrating Palmer drought severity index. *J Clim* 17:2335–2351. [https://doi.org/10.1175/1520-0442\(2004\)017%3c2335:aspdsi%3e2.0.co;2](https://doi.org/10.1175/1520-0442(2004)017%3c2335:aspdsi%3e2.0.co;2).
- Zang C, Biondi F. 2015. treeclim: an R package for the numerical calibration of proxy-climate relationships. *Ecography* (Cop) 38:431–436. <https://doi.org/10.1111/ecog.01335>.

Springer Nature or its licensor (e.g. a society or other partner) holds exclusive rights to this article under a publishing agreement with the author(s) or other rightsholder(s); author self-archiving of the accepted manuscript version of this article is solely governed by the terms of such publishing agreement and applicable law.